2012-06

Microelectromechanical systems bimaterial terahertz sensor with integrated metamaterial absorber

Alves, Fabio; Grbovic, Dragoslav; Kearney, Brian; Karunasiri, Gamani

Microelectromechanical systems bimaterial terahertz sensor with integrated metamaterial absorber

Fabio Alves, Dragoslav Grbovic, Brian Kearney, and Gamani Karunasiri*

Department of Physics, Naval Postgraduate School, 833 Dyer Road, Monterey, California 93943, USA
**Corresponding author: gkarunas@nps.edu*

Received January 26, 2012; revised February 24, 2012; accepted February 27, 2012;
posted February 28, 2012 (Doc. ID 162140); published May 21, 2012

This Letter describes the fabrication of a microelectromechanical systems (MEMS) bimaterial terahertz (THz) sensor operating at 3.8 THz. The incident THz radiation is absorbed by a metamaterial structure integrated with the bimaterial. The absorber was designed with a resonant frequency matching the quantum cascade laser illumination source while simultaneously providing structural support, desired thermomechanical properties and optical readout access. Measurement showed that the fabricated absorber has nearly 90% absorption at 3.8 THz. A responsivity of 0.1°/μW and a time constant of 14 ms were observed. The use of metamaterial absorbers allows for tuning the sensor response to the desired frequency to achieve high sensitivity for potential THz imaging applications.

OCIS codes: 040.2235, 160.3918.

THz imaging in 1–10 THz has been demonstrated using conventional, microbolometer-based imagers optimized for infrared (IR) wavelengths (8–12 μm) coupled with a quantum cascade laser (QCL) as an illumination source [1,2]. Since the background thermal energy in the THz range is small compared to that of infrared (IR) for passive imaging, THz imaging schemes usually employ a source to illuminate the target. However, microbolometer cameras are not optimized to operate in the THz range due their small pixel size (~25 μm) relative to THz wavelengths (~100 μm) and the pixel membrane is not designed for high THz absorption. Similar limitations also apply to micromechanical bimaterial-based IR imaging technology [3,4], which is another possible candidate for THz imaging.

Both approaches rely on thermal detection where the absorbed electromagnetic radiation heats the sensing element, changing its resistance in the case of microbolometers, and deforming its structure in the case of bimaterial sensors. Although both approaches share the same detection principle, bimaterial sensors appear to be more attractive as a research platform due to the possibility of utilizing external optical readouts [5,6], eliminating the requirement of monolithic integration of readout electronics [7]. To achieve high sensitivity in the THz spectral range, it is necessary to design pixels featuring high THz absorbing materials and to optimize their size for the desired spatial resolution.

One approach to achieve high THz absorption is to employ metamaterial structures, which can be fabricated using standard microfabrication materials. Several groups have reported the analysis and fabrication of metamaterial structures operating in THz spectral band using a variety of configurations, including resonant elements and periodic arrays of metallic squares and rings [8–11].

A recent work demonstrated a micromechanical sensor operating in microwave and sub-terahertz frequencies using a single split-ring resonator with simulated absorption of around 40% [12]. In this Letter, we describe fabrication of an uncooled bimaterial THz sensor with integrated metamatrial absorber having nearly 90% absorption at 3.8 THz, the same frequency emitted by the illuminating quantum cascade laser (QCL) source available to us.

The designed detector, shown in Fig. 1, is comprised of two main regions: (a) a metamaterial terahertz absorber, which is responsible for converting the absorbed THz radiation into heat and also providing good reflection in the visible range for the optical readout; and (b) multifold bimaterial microcantilevers (legs) responsible for deflecting the overall structure due to a temperature increase resulting from the heat generated by THz absorption. The legs are anchored to the substrate, which acts as a heat sink, allowing the sensor to return to its unperturbed position when excitation is terminated. The above requirements, coupled with the need for compatibility with the microelectromechanical systems (MEMS) fabrication process, put additional constraints on the materials used in the fabrication of bimaterial pixels. In our design, we benefitted from the favorable combination of thermal, mechanical, and optical properties of SiO_2 and Al [4], which make them ideal for building structures with high THz absorption as well as large bimaterial deflection, while remaining MEMS fabrication-friendly.

The metamaterial absorber is designed to have peak absorption at 3.8 THz, which is the lasing frequency of the QCL available to us [13]. The concept was demonstrated for microbolometers in the IR range [14] and our design consists of an array of Al squares (16.5 μm)

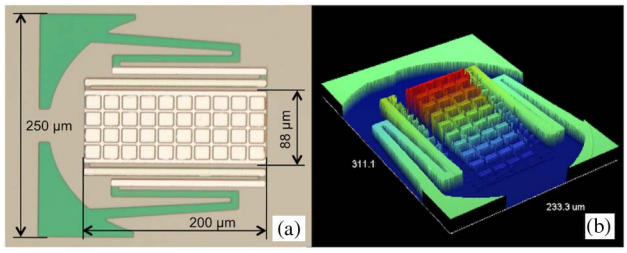

Fig. 1. (Color online) (a) Micrograph of the bimaterial MEMS sensor before releasing and (b) optical profilometry profile of the released pixel. It can be seen in (b) that the pixel membrane is deformed due to residual stress.

with periodicity of 20 μm separated from an Al ground plane by a SiO_2 layer. The Al and SiO_2 layers are about 100 nm and 1.2 μm thick, respectively. The absorbing area of the pixel is 88×200 μm^2 and contains 40 Al squares to form the metamaterial structure.

The THz detectors were fabricated using standard micromachining technology. First, a 100 nm thick aluminum (Al) film is deposited on a 300 μm thick silicon (Si) substrate. Then, the Al layer is patterned using photolithography and sputter-etched to form the absorber array and the first pair of aluminized legs (closest to the absorber). Next, a 1.2 μm thick silicon dioxide (SiO_2) layer is deposited using plasma enhanced chemical vapor deposition (PECVD) at 300 °C, followed by another 100 nm thick Al film.

The second metal layer is then patterned using photolithography and wet etched to define the absorber ground plane (which also acts as a reflector for the optical readout of deformation due to the heat generated from THz absorption) and the second pair of aluminized legs with Al on the opposite side. The sensor structure is then patterned by reactive ion etching the SiO_2 layer to define the pixel as shown in Fig. 1(a). The two outer arms of the folded leg on each side attached to the substrate (in green) do not have Al and provide thermal insulation to the pixel. Finally, the structures were released through backside trenching using the Bosch etch process. The profile of a released pixel measured using optical profilometry is shown in Fig. 1(b), where the deformation of the pixel membrane is due to residual stress after fabrication. Such a deformation does not affect the sensitivity of the sensor and can be minimized by further refining the fabrication process.

The absorption properties of the metamaterial structure were simulated using COMSOL multiphysics software, a three-dimensional finite element modeling program, and are shown by the dashed line in Fig. 2. The index of refraction of SiO_2 at THz frequencies was taken from [15] as $2.0 + 0.025i$ and a conductivity of 1×10^7 S/m was used for Al. The spectral characteristics of the fabricated metamaterial were measured using a Fourier transform infrared spectrometer (FTIR) extended to THz range and appropriate accessories. The measured absorption is shown in Fig. 2 (dotted line) along with the QCL source emission characteristics (solid line). Note that the laser frequency matches well with the maximum absorption of the metamaterial structure. Good agreement between measured and simulated absorption spectra indicates that the finite element modeling approach employed can be used to design metamaterial absorbers with the desired spectral characteristics.

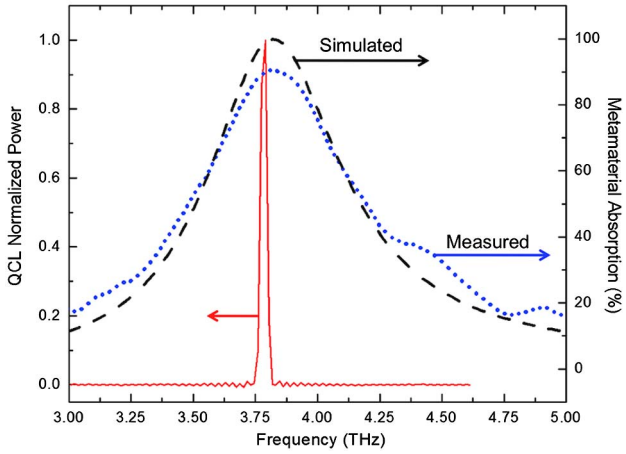

Fig. 2. (Color online) Measured (dotted curve) and simulated (dashed curve) absorption spectra of the metamaterial structure. Note that the peak absorption matches well with the measured QCL emission frequency (solid curve).

The thermal response of the sensor was obtained by attaching it to a heating element and using a linear photodiode array (linear positioning system) to measure the deflection of a HeNe laser beam reflected by the pixel. Figure 3 shows the measured angular displacement of the pixel membrane as a function of temperature.

The angular displacement is nearly linear with a negligibly small hysteresis. The measured thermal response is comparable to that in [4] for similar structures (without a metamaterial absorber) employed as an infrared sensor. The angular displacement can be further increased by optimizing the aluminum and SiO_2 layers thicknesses on the legs.

An important parameter for imaging applications is the sensor's operation speed. This parameter was measured using the same procedure used in the thermal response, except that the sensor was placed in a vacuum chamber to reduce convection heat loss. The THz beam from the QCL was directed to the detector using a combination of two off-axis parabolic mirrors. The inset in Fig. 4 shows the temporal response of the sensor when the QCL power supply is gated using a square pulse generator operating at 1 Hz. The measurement clearly shows that the absorption of THz from the laser deflects the pixel membrane. The sensor's operation speed was also measured by changing the gating rate of the power supply as shown in Fig. 4, which indicates that the sensitivity of the pixel diminishes beyond about 100 Hz. The 3 dB cutoff frequency was found to be around 11 Hz, giving a time constant of about 14 ms, which is in the same ballpark as microbolometer infrared detectors [16].

The speed of the sensor is primarily limited by the thermal time constant (τ), which is given by the ratio between the heat capacitance (C) and the thermal conductance (G) [16]. The thermal capacitance of the sensor was

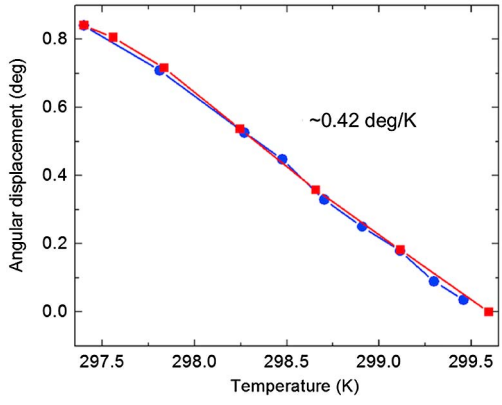

Fig. 3. (Color online) Angular deflection of the pixel membrane as a function of temperature by heating it under ambient conditions.

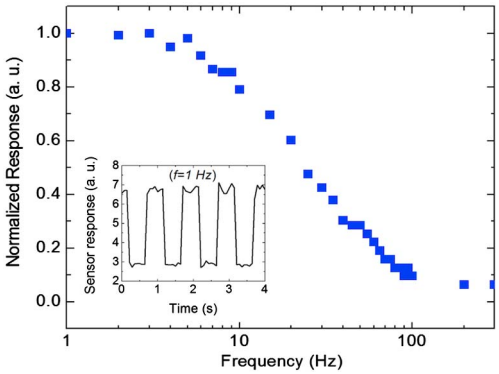

Fig. 4. (Color online) Speed of operation of the sensor measured by sweeping the gating frequency of the QCL power supply. The inset shows the temporal response of the detector at 1 Hz.

estimated using the dimensions and specific heat capacitance of the materials and found to be about 5.5×10^{-8} J/K. The thermal conductance of the sensor consists of heat losses via the legs, radiation and convection. Using the measured thermal time constant and estimated heat capacitance, the thermal conductance of the sensor was estimated to be about 3.9×10^{-6} W/K. The responsivity, R, of a bimaterial sensor can be defined as angular deflection per unit incident power ($d\theta/dP$), which is equal to (η/G) ($d\theta/dT$). The fraction of incident power absorbed by the sensor, η, is approximately 0.9 based on the data in Fig. 2 and the slope of angular deflection with temperature ($d\theta/dT$) can be extracted from Fig 3. Therefore, the estimated sensor peak responsivity is about 0.1 deg /μW, comparable to the responsivity of infrared bimaterial sensors reported in [4]. The intrinsic angular deflection noise of the sensor was estimated using the approach in [4] and found to be about 4 μdeg. However, the measured noise, including that generated by the optical readout system, was found to be about 175 μdeg, confirming that the sensor currently is not the limiting factor. The responsivity of the sensor can be further increased by changing the Al/SiO_2 thickness ratio to optimize the bimaterial deflection. It is important to note that responsivity and speed of operation are inversely proportional.

Higher deflection implies smaller thermal conductance and, consequently, a larger time constant. The specific application will determine what the optimal balance between these parameters is. Furthermore, modifying the dimensions of the metamaterial unit cells can also modify the absorption spectral characteristics, tuning the peak absorption to the desired frequency [14]. This flexibility in design demonstrates that MEMS bimaterial sensors can be fabricated for imaging at specific THz frequencies tuned to the illuminator.

In summary we have demonstrated a bimaterial MEMS sensor with integrated metamaterial absorbers operating at 3.8 THz. The absorption characteristic of the fabricated metamaterial structure agrees well with that of the simulations and the peak absorption is matched with the emission line of the QCL at 3.8 THz. The speed of operation of the sensor was found to be limited by the thermal time constant. The response of the sensor can be further enhanced by optimizing the pixel structure for fabrication of focal plane arrays to be used in active THz imaging.

This work is supported by a grant from the Office of Naval Research (ONR). The authors would like to thank E. Dupont, R. Ng, N. Lavrik, and S. Barone for technical assistance. This research was conducted at the Center for Nanophase Materials Sciences, which is sponsored at Oak Ridge National Laboratory by the Scientific User Facilities Division, Office of Basic Energy Sciences, U.S. Department of Energy.

References

1. W. M. Lee, B. S. Williams, S. Kumar, Q. Hu, and J. L. Reno, IEEE Photon. Technol. Lett. **18**, 1415 (2006).
2. N. Behnken, G. Karunasiri, D. R. Chamberlin, P. R. Robrish, and J. Faist, Opt. Lett. **33**, 440 (2008).
3. F. Dong, Q. Zhang, D. Chen, L. Pan, Z. Guo, W. Wang, Z. Duan, and X. W. Dong, Sens. Actuators A **133**, 236 (2007).
4. D. Grbovic, N. V. Lavrik, S. Rajic, and P. G. Datskos, J. Appl. Phys. **104**, 054508 (2008).
5. Q. Zhang, Z. Miao, Z. Guo, F. Dong, Z. Xiong, X. Wu, D. Chen, C. Li, and B. Jiao, Optoelectron. Lett. **3**, 119 (2007).
6. H. Tao, N. I. Landy, C. M. Bingham, X. Zhang, R. D. Averitt, and W. J. Padilla, Opt. Express **16**, 7181 (2008).
7. J. Cao, Z. Chen, W. Lu, Y. Zhang, K. Lei, and B. Zhao, Proc. SPIE **7383**, 73834J (2009).
8. H. T. Chen, J. F. O'Hara, A. K. Azad, and A. J. Taylor, Laser Photon. Rev. **5**, 513 (2011).
9. Y. Ma, Q. Chen, J. Grant, S. C. Saha, A. Khalid, and D. R. S. Cumming, Opt. Lett. **36**, 945 (2011).
10. H. Mosallaei and K. Sarabandi, in *Proceedings of 2005 IEEE Antennas and Propagation Society International Symposium*, **1B** (IEEE, 2005), pp. 615–618.
11. H. Luo, Y. Z. Cheng, and R. Z. Gong, Eur. Phys. J. B **81**, 387 (2011).
12. H. Tao, E. A. Kadlec, A. C. Strikwerda, K. Fan, W. J. Padilla, R. D. Averitt, E. A. Shaner, and X. Zhang, Opt. Express **19**, 21620 (2011).
13. S. Fathololoumi, D. Ban, H. Luo, E. Dupont, S. R. Laframboise, A. Boucherif, and H. C. Liu, IEEE J. Quantum Electron. **44**, 1139 (2008).
14. T. Maier and H. Bruckl, Opt. Lett. **34**, 3012 (2009).
15. Y. Smith, E. Shiles, and M. Inokuti, in *Handbook of Optical Constants of Solids*, E. D. Palik, ed. (Academic, 1998), pp. 306–406.
16. R. A. Wood, Semicond. Semimet. **47**, 43 (1997).